EFFECT OF GRINDING ON THE FATIGUE STRENGTH OF A BEARING STEEL IN THE SUPER LONG-LIFE FIELD

M. Goto[1], T. Yamamoto[1], H. Nisitani[2], T. Sakai[3] and N. Kawagoishi[4]

[1] Dept. of Mechanical Eng., Oita University, Oita, 870-1192, Japan
[2] Dept. of Mechanical Eng., Kyushu-Sangyo University, Fukuoka, 813-8577, Japan
[3] Dept. of Mechanical Eng., Ritsumeikan University, Kusatsu, 525-8577, Japan
[4] Dept. Mechanical Eng., Kagoshima University, Kagoshima, 890-0065, Japan

ABSTRACT

In order to study the fatigue damage of a high carbon chromium steel SUJ2, rotating bending fatigue tests of smooth specimens (K_t = 1.06, stress concentration factor) were carried out. The specimens were finished by the grinding after the heat-treatment. The fatigue strength of EP-0 (ground) specimen exhibited large scatter and it tended to drop again in the long-life field in excess of 10^7 cycles. In such a case, fish-eye was left on the fracture surface. In order to study the effect of surface hardened layer due to the grinding, two types of EP (electropolished) specimens, EP-15 specimen whose surface hardened layer and grinding flaws were almost removed and EP-3 specimen which has the decreased surface roughness and surface hardened layer, were fatigued. The fatigue strength of EP-15 specimen was dramatically decreased when compared to the EP-0 specimen, and no drop in fatigue strength in the long-life field was observed. This indicates that the drop in fatigue strength in the long-life field results from the surface strengthened layer due to the grinding. On the other hand, S-N data of EP-3 specimen exhibited large scatter, but the range of scatter was smaller than that of EP-0 specimen. This narrowed scatter may be related to the decreased surface roughness of EP-3 specimen. In addition to the fatigue tests, the measurements of surface hardness, residual stresses, surface roughness and SEM observation of fracture surface were carried out for each type of the specimen. Considering the experimental results synthetically, the physical basis of peculiar S-N characteristics of ground specimen was investigated.

INTRODUCTION

It has been reported that the fatigue strength of high strength steels and surface strengthened steels tends to decrease in the long-life field in excess of $N = 10^7$ cycles [1-5]. In such a super long-life field, the starting point of fracture was principally the non-metallic inclusions which located inside the specimen. On the other hand, some machines and structures have been operated for long time beyond their design life. This indicates that the members designed on the basis of fatigue limit stress at 10^7 cycles lose the reliability for safety in the super long-life field. Thus, it is crucial to evaluate the fatigue strength in the super long-life field for increased safety of high-strength steels operating for long time.

As the manufacturing process of the specimen for high-strength steels, the surface finish due to the grinding after the heat-treatments is generally accepted. This means that the hardened layer, residual stresses and grinding flaws are left on the surface as a result of grinding. Fatigue cracks are usually initiated from the surface and the initial cracks propagate in such a affected surface layer. Also, the crack starting point may shift to the inside the specimen as is indicated for the surface hardened materials. Thus, the effect of grinding

on the fatigue behaviour should be clarified for evaluation of fatigue damage of high-strength steels.

In order to study the fatigue damage of a high carbon chromium bearing steel SUJ2, rotating bending fatigue tests of smooth specimens (K_t = 1.06, stress concentration factor) were carried out. The specimens were finished by the grinding after the heat-treatment. In addition to the fatigue test of the ground specimens, to study the effect of surface affected layer due to the grinding, two types of electropolished specimens; the specimen whose surface hardened layer and grinding flaws were almost removed (15 μm electropolishing) and another is the specimen which had the decreased surface roughness and surface hardened layer (3 μm electropolishing), were fatigued. After the fatigue tests, fracture surface was analysed by SEM. The effect of grinding on the fatigue strength over till giga-cycles was investigated based on the experimental results.

EXPERIMENTAL PROCEDURES

Material used was a high carbon chromium steel for the use of bearing (JIS Material Code: SUJ2). The chemical composition (wt %) was 1.01 C, 0.23 Si, 0.36 Mn, 0.012 P, 0.007 S, 1.45 Cr, 0.06 Cu, 0.04 Ni, 0.02 Mo, remainder ferrite.

Figure 1 shows the shape and dimensions of the specimen. After the machining of the specimen, the specimens were heat-treated, quenching (835•, 40 min•oil cooling) followed by tempering (180•, 120 min•air cooling). Figure 2 shows the microstructure of the material. Ultimate tensile strength was 2316 MPa. The round notch surface was polished by a grinder having a mesh of #100 after the heat-treatment. Notch radius is 7 mm and the stress concentration factor of this geometry is 1.06. The specimens finished up by the grinding are called EP-0 specimen, EP-0 means no (0 μm) electropolishing. For some EP-0 specimens, in order to study the effect of surface affected layer due to the grinding, two types of electropolishing; one is 15 μm electropolishing to remove the surface hardened layer and grinding flaws; and another is 3 μm electropolishing to obtain the decreased surface roughness and surface hardened layer, were carried out. The electrolyte was made by mixing 1000 g phosphoric acid, 20 g oxalic acid dihydrate and 20 g gelatin.

All the test were carried out using a cantilever-type rotating bending fatigue machine operating at 3150 rev/min. This machine has two spindles driven by an electric motor via a flat belt, and each spindle has specimen grips at both ends. Namely, fatigue tests of four specimens can be performed simultaneously. The value of stress, σ_a, was defined by the maximum stress amplitude at the minimum cross section. The observation of fracture surface was made by SEM.

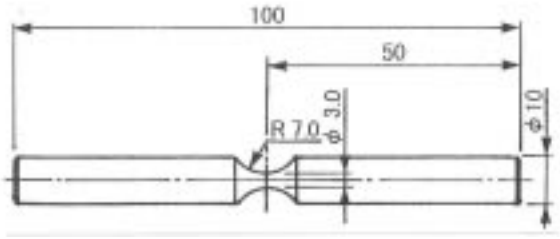

Figure 1: Shape of the specimen (in mm)

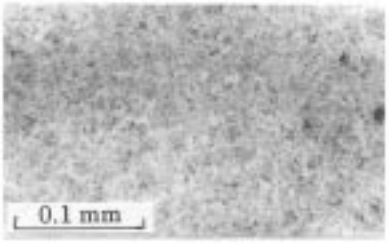

Figure 2: Microstructure of the material

EXPERIMENTAL RESULTS AND DISCUSSION

S-N Characteristics of Ground (EP-0) Specimens

Ordinary fatigue tests were conducted to get the S-N characteristics of the EP-0 specimen. Fatigue limit stress was calculated by the staircase method using ten specimens. The number of cycles for run-out was 10^7 cycles. The specimens survived after 10^7 cycles were fatigued uninterruptedly at the same stress amplitude. Figure 3 shows the S-N curve. The fatigue limit stress at 10^7 cycles: σ_{w0}, which is characterized by a horizontal line in the figure, is 1200 MPa (s = 31.08 MPa, s: standard deviation). At the number of cycles in excess of 10^7 cycles, fatigue strength exhibits a decreasing trend. For example, a specimen fatigued under σ_a

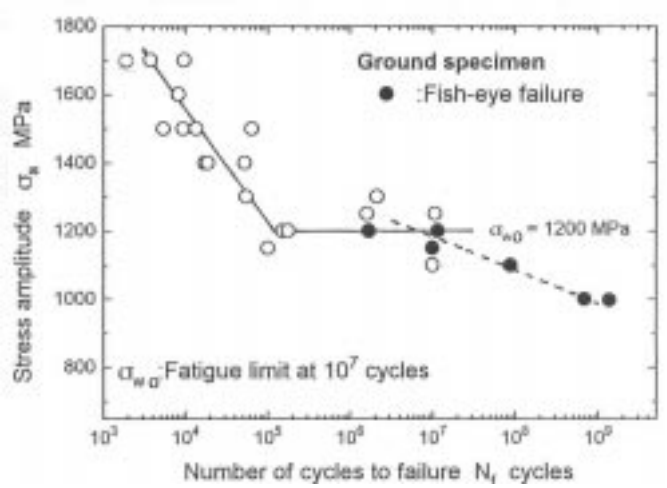

Figure 3: S-N Characteristics of EP-0 (ground) specimen

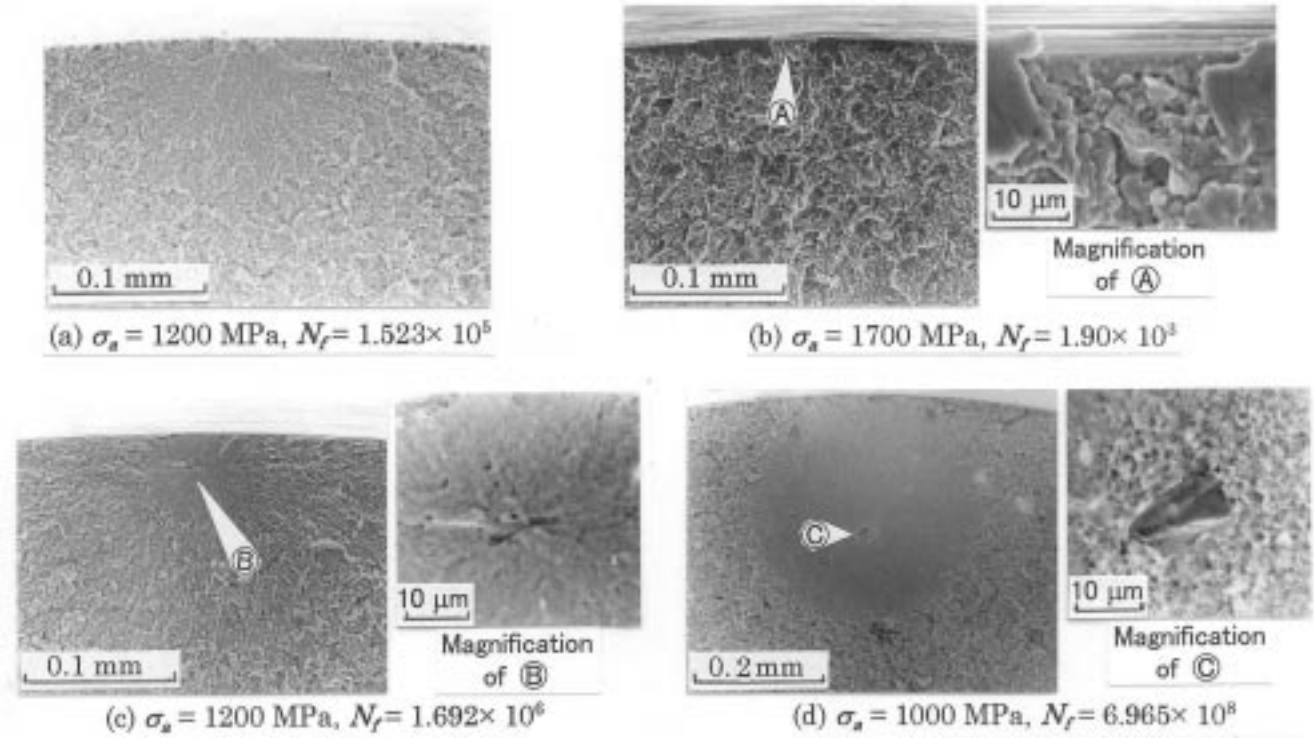

Figure 4: SEM observations of fracture surface for the EP-0 specimens

= 1000 MPa was fractured over giga-cycles (N_f = 1.36×10^9). This indicates that the peculiar S-N characteristics exists in the long life field in excess of 10^7 cycles.

In order to study the physical basis of the S-N characteristics, the fracture surface of all the specimens was inspected by SEM. Figure 4 shows the typical fracture surfaces. For the case of (a), the starting point of a crack is surface where no small defects are observed. A crack may be initiated from crystalline slip at the surface. Case (a) was the typical surface fracture mode, however, another surface fracture mode shown in (b) was also observed. The crack initiation site in this case is at the bottom of the grinding flaws. On the other hand, the crack starting sites for (c) and (d) are interior defects and the fish-eye pattern is left on the fracture surface. The non-metallic inclusion is recognized near the center of fish-eye. The average sizes of inclusions were about 10 μm. Open and solid symbols in Fig.3 indicate the specimen fractured from the surface and interior defect, respectively. Thus, it is roughly concluded that the fracture in the short-life field (N_f <10^6) is from the surface, and the fracture in the long-life field (N_f >10^6) is from the interior defect. At a stress around fatigue limit σ_{w0}, however, the surface fracture mode is frequently observed for the specimens fractured at a large number of cycles (N_f >10^6).

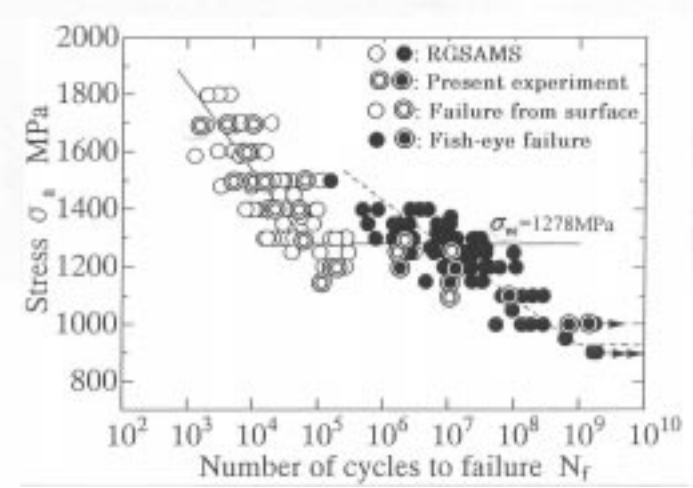

Figure 5: S-N characteristics given by the RGSAMS (•,•:present experiment)

Figure 5 shows the S-N characteristics of the ground specimen by RGSAMS (Research Group of Statistical Aspect of Material Strength) [4]. For the sake of comparison, the present data (Fig.3) are also plotted by the •,• symbols. The RGSAMS is proceeding the projects on the super high-cycle fatigue of the high-strength steels. Over 30 institutes join the project to gather the large volume of super high-cycle fatigue data, and the RGSAMS supplies the same specimen and fatigue machine. The present experiment of the ground specimen is included in the project. Figure shows that there are no significant difference in fatigue strength between the present experiment and the RGSAMS. In general, it is found that the fatigue strength of ground specimen exhibits large scatter and it tends to drop again in the long-life field in excess of 10^7 cycles. In such a long-life field, a crack tended to initiate from an interior non-metallic inclusion (the fish-eye pattern was left on the fracture surface).

Effect of Removing Surface Layer on Fatigue Strength

As the effect of grinding, (i) an increase in hardness of the surface layer, (ii) the compressive residual stresses, (iii) the notch effect of a grinding flaw, and (iv) the change in material property are considered. In what follows, paying particular attention to the terms (i) to (iii), the influence of grinding on the fatigue strength is studied based on the experimental results obtained from the two types of electropolished specimens; EP-15 whose surface hardened layer and grinding flaws were almost removed; and EP-3 which had the decreased surface roughness and surface hardened layer.

Figure 6 shows (a) the micrograph of surface and (b) the surface roughness measured along the axial direction. The $\boldsymbol{R_{max}}$ values are 6.36, 1.96 and 0.64 μm for EP-0, EP-3 and EP-15 specimen, respectively. The surface roughness is averaged by electropolishing, in other words, the scatter in geometrical shape of surface tends to be reduced with an increase in electropolishing.

Table 1 shows the value of residual stresses measured at the midsurface of the specimen. The compressive residual stresses over -500 MPa is produced in axial direction for EP-0 specimen. It is about -360 MPa for EP-3, but is about 80 MPa for EP-15. Consequently, the compressive residual stresses nearly disappear due to electropolishing of 15 μm surface layer.

Table 1: Residual stresses measured at the specimen surface

Specimen	Residual stresses MPa	
	Axial direction	Circumferential direction
EP-0 (ground)	- 517	- 429
EP-3	- 364	- 269
EP-15	79	- 74

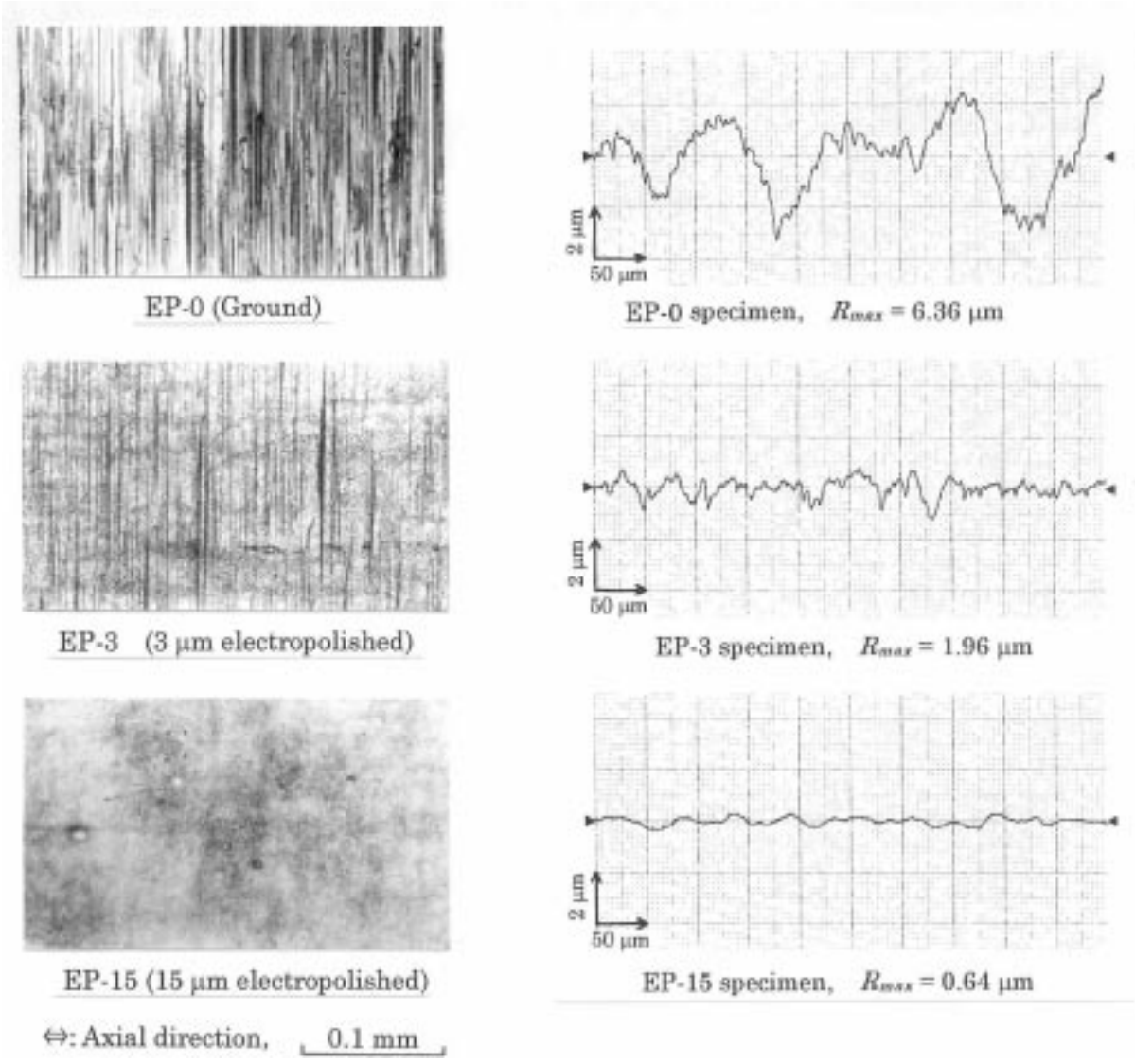

(a) Micropraph of the surface (b) Surface roughness

Figure 6: Surface morphology and roughness for each specimen

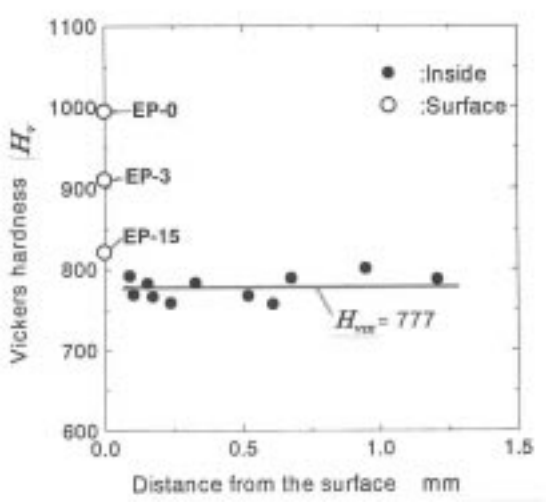

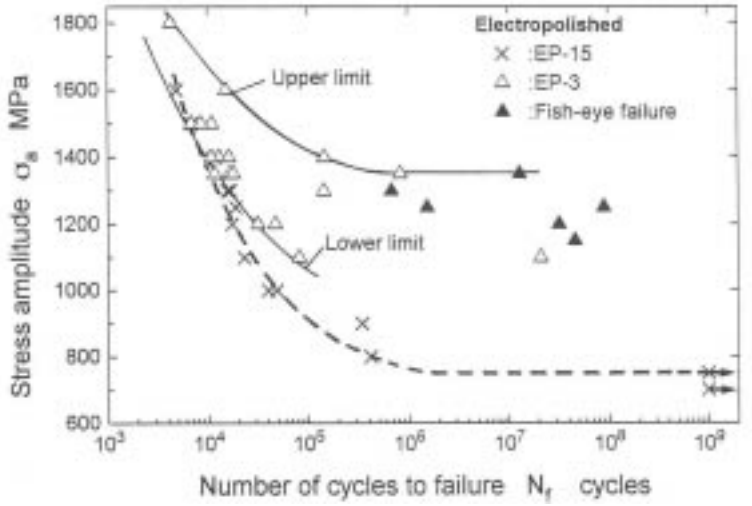

Figure 7: Distribution of the hardness **Figure 8:** S-N characteristics of electropolished specimens

Figure 7 shows the Vickers hardness number measured over the cross section and at the surface. The load used was 2.94 N. The hardness of cross section distributes flat from 0.1 mm below the surface to the centre of the specimen. The average hardness is H_{vm} = 777. On the other hand, the surface hardness for each

specimen is H_v = 995, 910 and 821 for EP-0, -3 and -15, respectively. This suggests that the surface layer less than 20 μm is strengthened strongly by the grinding.

Figure 8 shows the S-N characteristics of EP-3 and -15 specimen. The fatigue strength of EP-15 specimen is dramatically decreased when compared to EP-0, and distinct fatigue limit stress exists (σ_{w15} = 750 Mpa • $0.63\sigma_{w0}$). The scatter in fatigue data is relatively small. This indicates that the scatter in material property caused by the heat-treatment was not large. Therefore, tremendously large scatter in S-N plots for EP-0 specimen is derived from the grinding finish. Figure 9 (a) shows the fracture surface of EP-15. All the cracks of EP-15 were initiated from the surface. On the other hand, the scatter in S-N plots of EP-3 specimen is larger than EP-15. Figures 9 (b), (c) and (d) show the fracture surfaces of EP-3. All the fracture origins in the short-life field ($N_f < 10^5$) were at the surface: (b). In the long-life field ($N_f > 10^6$), however, the fracture origins were inside the specimen: (c), excepting one specimen fractured from the surface grinding flaw (N_f = 2.102×10^7,depth of flaw is 2.5 μm): (d). In Fig.8, the • symbol means the fish-eye failure and the two full lines indicate the upper and lower limits of S-N plots for EP-3. Lower limit line is close to the S-N curve of EP-15. Figure 10 shows the crack initiation site of EP-3 specimen fractured at the lower limit line. Although the grinding flaws exist over the whole surface, no extraordinary rough flaws and defects are observed at the crack initiation site.

Figure 11 shows the comparison of the scatter band (the upper and lower limits of S-N plots) between EP-3 and EP-0 specimen. The range of scatter in fatigue strength is smaller in EP-3 than EP-0. This narrowed scatter may be related to the decreased surface roughness of EP-3. The geometric shape of surface is averaged by electropolishing. This indicates that the scatter in fatigue strength is decreased in EP-3 than EP-0. On the other hand, no significant large difference in average fatigue strength between EP-3 and EP-0 was observed (both the S-N plots roughly overlap each other, whereas its scatter is slightly smaller in EP-3). Removing surface layer by electropolishing produces the decreased surface hardness and compressive residual stresses, which decrease the fatigue strength. However, it produces the reduced surface roughness, which increases the fatigue strength. As the result of such opposite two actions, the fatigue strength of EP-3 specimen may roughly coincide with EP-0.

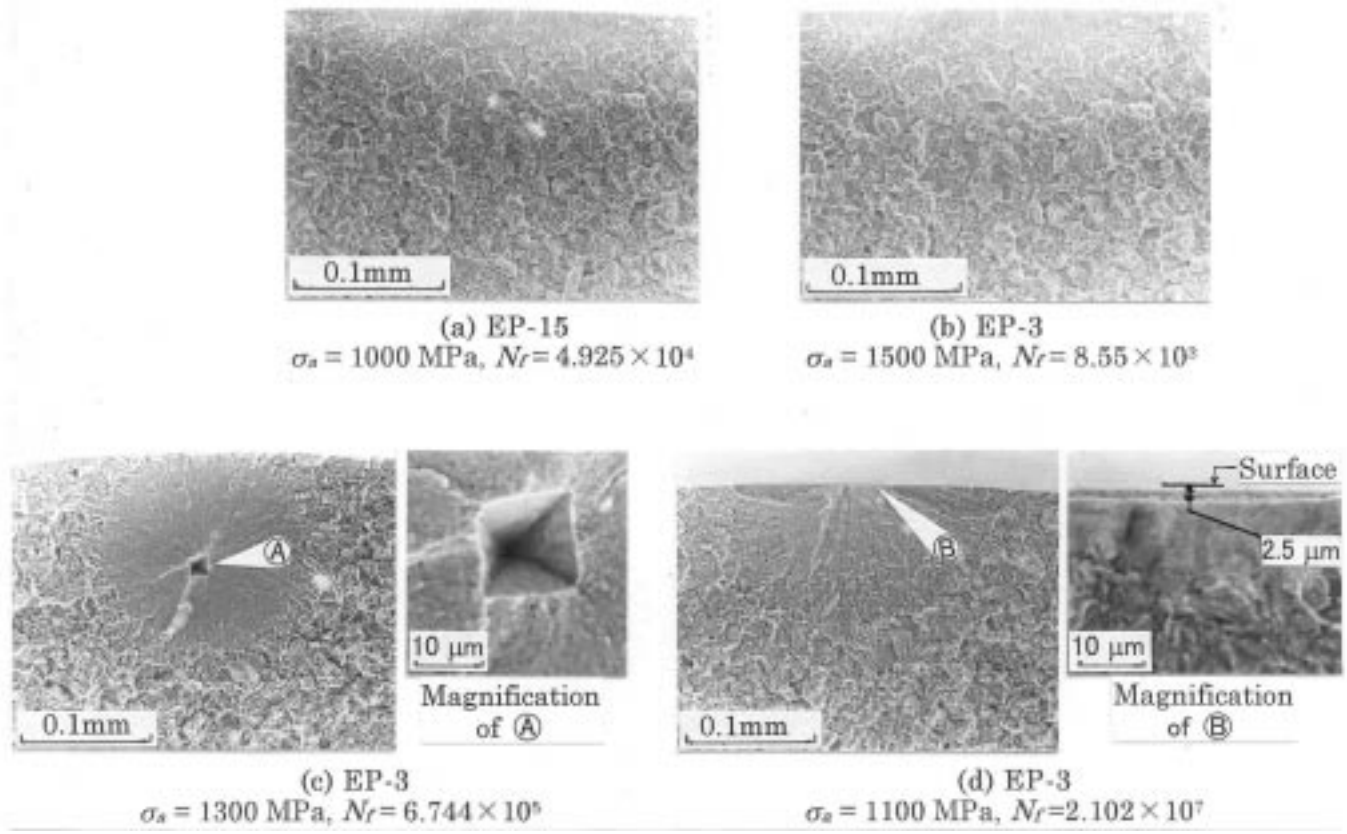

Figure 9: SEM observations of the fracture surface, (a) EP-15specimen and (b-d) EP-3 specimen

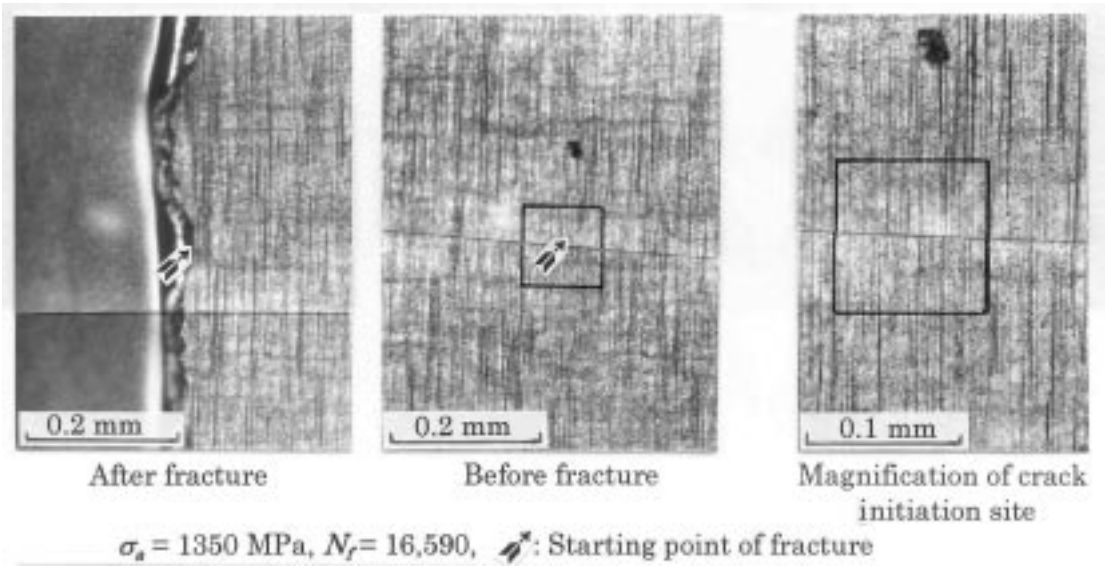

Figure 10: Crack initiation site of EP-3 specimen fractured at relatively small number of cycles

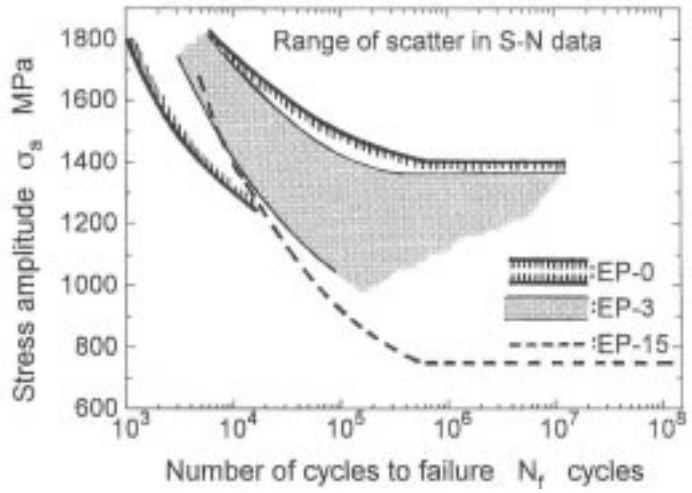

Figure 11: Comparison of scatter band of S-N data between the EP-0 and EP-3 specimens

S-N Characteristics of Ground Specimen and Surface Affected Layer

The ground specimen exhibits the peculiar S-N characteristics, namely the fatigue strength drops again in the long-life field in excess of 10^7 cycles. The phenomenon of re-drop in fatigue strength is closely related to the surface strengthened layer due to the grinding finish. After the grinding, the surface layer is plastically deformed. The plastic deformation produces the work hardening layer and compressive residual stresses. When the stress is loaded cyclically at this deformed layer, the microscopic situation of the surface layer is nearly equivalent to the fatigue tests of prestrained material with a mean stress. Considering the experimental results from the fatigue tests of prestraining and mean stresses [6-9], it can be infer that the work hardening makes increase the resistance for crack initiation and initial crack growth. As for the residual stresses, it may have no influence of crack initiation (it has been reported that the crack initiation life is not affected by the mean stress [8]), but it decreases the crack growth rate after the initiation. Thus, the fatigue strength of ground specimen is larger than the base material. Under the stresses below the fatigue limit of surface hardened layer, however, a fatigue crack initiates from an inner defect under the appropriate condition because of the less hardness of inside than the surface. It takes a great deal of times to initiate and propagate the inner cracks. Therefore, the re-drop of fatigue strength generally occurs in the long-life field. The experimental facts, that the fatigue strength of EP-15 is smaller that EP-0 and the fracture of EP-15 starts from the surface, support above statements. Consequently, the peculiar S-N characteristics observed in high-strength materials is not necessarily the proper phenomenon of the material itself.

With regard to the scatter in S-N plots for EP-0, the scatter is tremendously large even the case that the fracture origin is at the surface. The scatter in S-N plots decreases with an increase in the amount of electropolishing. The increase in removing surface layer due to electropolishing decreases the scatter in the geometric shape of surface. Accordingly, the large scatter in fatigue strength of ground specimen may principally derive from the scatter in grinding flaws.

The S-N plots of ground specimen shows that the different fracture modes exist together at around fatigue limit stress at 10^7 cycles (see Figs.2 and 4), whereas the surface fracture mode is liable to occur at a high stress (short-life field) and the inner fracture mode at a low stress (long-life field). This phenomenon may be closely related to both the scatters in surface roughness and inner defects. In other words, the sizes of the crucial grinding flaws and inner defects are different by individual specimen. Accordingly, when the ground specimens whose surface layer condition is perfectly controlled are fatigued, their fracture mode may be clearly divided into two mode at the fatigue limit stress of surface layer; surface fracture mode at a stress above the fatigue limit and inside fracture mode below the fatigue limit.

CONCLUSIONS

In order to study the fatigue damage of a heat-treated high carbon chromium steel SUJ2, rotating bending fatigue tests of EP-0, EP-3 and EP-15 specimens were carried out. Here, EP-0 means the specimen finished by the grinding, EP-3 and EP-15 are the specimens whose 3 and 15 μm surface layer were electropolished after the grinding, respectively. The main conclusions from analysis of fatigue data may be summarized as follows.

(1) The fatigue strength of EP-0 exhibited large scatter and it tended to drop again in the long-life field in excess of 10^7 cycles. The fracture origin in such a long life field was principally inner defects. At around the fatigue limit stress at 10^7 cycles, two different fracture modes, surface fracture and inclusion governed inside fracture, were mixed together.

(2) Fatigue strength of EP-15 was dramatically decreased and the scatter in S-N plots is very small when compared to the EP-0. All the cracks of EP-15 were initiated from the surface even at the stress below the fatigue limit at 10^7 for EP-0.

(3) S-N plots for EP-3 exhibited large scatter, but the range of scatter is smaller than EP-0. This may come from the decreased scatter in geometric shape of the surface by electropolishing. On the other hand, the difference in the mean value of S-N plots between EP-0 and EP-3 is not large. Removing 3 μm surface layer, the drop in fatigue strength due to the reduced hardened layer and the increase in fatigue strength derived from the decreased surface roughness may balance.

(4) Considering above experimental results synthetically, it can be concluded that the peculiar S-N characteristics observed in ground specimen results from the surface strengthened layer (work hardening and residual stresses) due to grinding. Those experimental facts indicates that the re-drop in fatigue strength in super long-life field frequently reported in high-strength material is not necessary the proper characteristics of material itself.

References

1. Naito, T., Ueda, H. and Kikuchi, M. (1984) *Metal Trans.* **15A**, 1431.
2. Masuda, C., Nishijima, S. and Tanaka, Y. (1986) *Trans. JSME* **52A**, 847.
3. Bathias, C. and Bonis, J. (1998). In: *Fracture From Defects*, pp.321, Brown,M.W., de los Rios, E.R. and Miller K.J. (Eds), Emas Publishing.
4. Sakai, T., Takeda, M., Shiozawa, K., Ochi, Y., Nakajima, M., Nakamura, T. and Oguma,N. (1999). In: *Fatigiue '99*, pp.573, Wu, X-R. and Wang Z-G. (Eds), Higher Education Press and Emas Publishing.
5. Goto, M., Yamamoto, Y., Sato, M., Yamada, S., Kawagoishi, N., Sakai, T. and Nishitani, H.(1999). In:
   Advanced Mater. Develop. & Performance, pp.89, Nakabayashi, I. and Murakami. R.(Eds), Tokushima.
6. Frost, N.E. (1958) *Metallurgia* **57**, 279.
7. Maddox, S. J. (1975) *Int. J. Fracture* **11**, 389.
8. Nishitani, H. and Goto, M. (1984) *Trans. JSME* **50A**, 1926.
9. Goto, M., Yamamoto, T., Nisitani, H. and Kawagoishi, N.(1998), In: *Small Fatigue Cracks*,

Mech. and Applications, pp.207, Ravichandran K.S., Ritchie, R.O. and Murakami, Y. (Eds) Elsevier.